Composites Part C: Open Access 12 (2023) 100421

Contents lists available at ScienceDirect

Composites Part C: Open Access

journal homepage: www.sciencedirect.com/journal/composites-part-c-open-access

Parametric investigation of flexural performance of concrete prisms retrofitted with near-surface mounted FRP bars

Mohammad Al-Zu'bi [a], Mizi Fan [a,*], Lorna Anguilano [b]

[a] Department of Civil and Environmental Engineering, College of Engineering, Design and Physical Sciences, Brunel University London, UB8 3PH, United Kingdom
[b] Experimental Techniques Centre, College of Engineering, Design and Physical Sciences, Brunel University London, United Kingdom, UB8 3PH

ARTICLE INFO

Keywords:
Concrete members
Flexural retrofitting
NSM-FRP technique
Parametric study

ABSTRACT

This study investigates the impact of flexural retrofitting on the load-bearing capacity, ductility and failure modes of concrete prisms using the NSM-FRP technique, considering four design parameters. Some specimens were retrofitted with NE only, while others incorporated FRP (i.e. CFRP, GFRP or BFRP) reinforcement bars alongside NE to assess the influence of presence of FRP reinforcement on the specimens' performance. The study also examines changing the position of GFRP reinforcement bars (cantered or along the groove's edge), using different numbers of CFRP bars (one, two or three) and considering three groove dimensions (8×8 mm^2, 10×10 mm^2 and 12×12 mm^2). Results showed that NE-only retrofitting increased the capacity by about 38 % compared to the non-retrofitted specimens, with negligible impact on ductility. Introducing FRP reinforcement led to an approximately twofold increase in capacity and ductility compared to NE-only retrofitting. Placing GFRP reinforcement bars along the edge of the groove minimally affected the capacity but reduced ductility by about 24 %. Increasing the number of CFRP bars from one to three significantly improved capacity and ductility but increased the risk of debonding failures. Using larger groove sizes (10×10 mm^2) enhanced capacity of the CFRP-retrofitted specimens, slightly reduced GFRP-retrofitted concrete capacity and improved ductility for both. The 12×12 mm^2 groove size reduced capacity but increased ductility. The 10×10 mm^2 groove size effectively prevented debonding failures observed with other sizes.

1. Introduction

Despite numerous successful concrete structures, many have been compromised and rendered unsafe or unsatisfactory for current specifications, because of corrosion of steel reinforcement, improper/insufficient maintenance, severe environmental conditions, increase in the applied loads recommended by design codes and standards due to functional change and/or errors in the design/construction phase [1–4]. All these reasons would negatively affect the durability and serviceability of concrete structures and deteriorate their structural integrity. Therefore, the need for retrofitting is gradually increasing with the increase of the age of concrete structures.

Using fibre reinforced polymer (FRP) materials has gained popularity worldwide in retrofitting applications and civil construction since the 1990s and could produce reliable strengthening and repairing systems for existing concrete structures [5–9]. This was due to continuing drops in the cost of those materials besides their many advantages over conventional strengthening materials (e.g. concrete, steel and wood), including their high strength-to-weight ratio (i.e. high modulus of elasticity and tensile strength), low thermal conductivity, high durability (noncorrosive), electromagnetic neutrality, rapid execution with less labour, ease of handling. Furthermore, FRP reinforcements provide lower installation and reduced maintenance costs, reduced mechanical fixing, excellent malleability and unlimited availability in size (i.e. dimensions) and geometry.

Several techniques can be adopted to utilise the FRP materials in rehabilitating deteriorated structures. The externally bonded reinforcement (EBR) strengthening system is the most widespread system for strengthening/retrofitting of concrete structures and has become a prevalent technique over the last two decades [10]. However, the EBR-FRP reinforcement has a number of limitations/disadvantages. For instance, the premature debonding of FRP composites from concrete surface, as they are susceptible to the risk of physical damage, fire and vandalism as a result of collision during stress transfer process, and humidity effect for being open to atmosphere, where EB FRP plates tend to debond at low strains, which eventually limits the ductility or

* Corresponding author.
E-mail address: mizi.fan@brunel.ac.uk (M. Fan).

https://doi.org/10.1016/j.jcomc.2023.100421

Available online 22 November 2023

moment redistribution to such an extent that guidelines often impede moment redistribution, leading to inefficient use of reinforcing material. The drawbacks of the EBR-FRP system (i.e. debonding failure) have led the researchers to search for an alternative to provide the retrofitted members with better performance under severe conditions and near surface mounted (NSM) technique has been found to be the most appropriate alternative.

NSM technique was found to have many advantages over EBR counterpart; The NSM-FRP reinforcement is embedded into slits cut onto the concrete substrate using an appropriate adhesive, that would protect it against harm resulting from acts of vandalism, fire, mechanical damage, harsh environment and ageing effects. Thus, the FRP materials are less prone to debond from concrete substrate. Moreover, the NSM retrofitting process requires no surface preparation work and, after cutting the thin slit, requires minimal installation time. Owing to its numerous features, NSM-FRP system has been found to be in effect for retrofitting concrete structures. It has been reported that utilising NSM-FRP reinforcement is feasible in enhancing the flexural strength, ductility and load-carrying capacity of concrete elements [11–17]. The flexural response of the NSM-FRP-retrofitted concrete members has been found to be influenced by several factors, e.g. the percentage of NSM-FRP reinforcements [14,16,18–21], groove size [17,21,22] and FRP reinforcement type [17,27], to name a few. Using two NSM-carbon FRP (CFRP) bars rather than one yielded about 25.6 % and 7.5 % increases in the yielding and maximum loads, respectively, which increased by about 11.7 % and 13 % when using NSM- glass FRP (GFRP) bars [14]. Nurbaiah et al. [18] reported that doubling the number of the GFRP rods increased the ultimate load of the strengthened beams by 34 %, but reduced the ultimate deflection by 41 %. In contrast to that, doubling the number of GFRP bars could increase both maximum load (30.7 %) and mid-span deflection (15.2 %) [20]. Further study [21] indicated that tripling the CFRP reinforcement area led to about 14.4 % increase in the maximum load, however, about 29 % reduction in the maximum deflection was observed. Doubling basalt FRP (BFRP) bars showed increment in the maximum load (26.4 %) and the corresponding maximum moment (26.3 %), however, 13.7 % reduction in the mid-span deflection at maximum load was observed [19].

For the influence of the type of the FRP reinforcement, the yield and ultimate loads of the CFRP-reinforced beams were found to be consistently higher than GFRP counterparts by 23 % and 19.7 %, respectively [17]. However, the mid-span ultimate displacement and ductility factor dropped by 45 % and 69 %, respectively, which resulted in higher steel strains, indicating lower utilization ratio of the FRP reinforcement. Abdallah et al. [27] found that using NSM-GFRP bars improved ductility by about 24 % compared with using CFRP bars. However, the load-carrying capacity of the NSM-GFRP-strengthened beams was about 77 % of those strengthened with CFRP bars, which also achieved higher stiffness.

The effect of the groove dimensions has also been attempted. It was reported that using smaller groove width (i.e. 1.5*FRP strip width (b_b) instead of 2.0b_b) resulted in 28 % higher load capacity and about 44 % ductility increase [21], which could also delay the debonding failure. Soliman et al. [17] found that the ultimate loads of the specimens strengthened with a groove size (i.e. depth) of 1.5d (d is the CFRP bar diameter) were about 8.33 % higher than those strengthened with 2.0d groove size. It's noteworthy that minimum groove dimensions of 1.5d_b (d_b is the FRP bar diameter) has been proposed by the ACI 440.2R-08 [28]. Thus, all the relevant work done considered that suggestion, which doesn't always have to be the optimum groove size.

Therefore, it can be remarked that the research effort that was dedicated to study the effect of the groove size, the type and percentage of the FRP reinforcement on the efficiency of the NSM-FRP concrete retrofitting is inadequate, while there have been limited studies examining the impact of these parameters on the efficiency of the NSM-FRP retrofitting process for concrete members, few have specifically investigated the performance of BFRP-retrofitted specimens or explored the effects of increasing NSM-CFRP reinforcement, along with the use of groove dimensions smaller than 1.5d_b.

Thus, further in-depth exploration is highly required. Moreover, in order to investigate the full potential of utilizing the NSM-FRP reinforcement for concrete retrofitting, the influence of other parameters should be considered, e.g. the position of the FRP reinforcement inside the grooves, which, to the best of the authors' knowledge, has not been studied yet. Therefore, with the aim of establishing a correlation between retrofitting parameters and structural performance to eventually develop the optimum retrofitting systems, this study investigates the effect of multiple parameters on the efficiency of the NSM-FRP retrofitting process. A series of concrete specimens (i.e. prisms) with dimensions of 50 × 50 × 200 mm were flexural retrofitted and tested under three-point bending. The parameters investigated include the presence of NSM-FRP reinforcement, its position inside the groove, number of NSM-FRP bars in addition to the groove size. The results were presented and analysed in terms of the structural behaviour (i.e. capacity and ductility) of tested specimens in addition to the accompanying failure modes.

2. Experimental programme

2.1. Test specimens

For the purpose of NSM-FRP retrofitting, a total of 11 concrete prisms with dimensions of 50 × 50 × 200 mm were prepared, each with three replicates, ten of which were cast and retrofitted with 6 mm diameter CFRP, GFRP or BFRP bars each alongside neat epoxy (NE) adhesive and the eleventh was retrofitted using NE only. One more specimen (three replicates) served as a control (non-retrofitted). The specimens to be retrofitted are shown in Fig. 1a. The following test parameters were considered for the purpose of this study:

- presence of FRP reinforcement: the effect of retrofitting the concrete specimens with NE only and with FRP (i.e. CFRP, GFRP and BFRP) bars alongside NE was investigated.
- position of FRP reinforcement: the GFRP reinforcement was installed into grooves in two different positions, e.g. in the centre of the groove or at its edge.
- number of FRP bars: specimens were retrofitted with either one, two or three CFRP bars.
- groove size: three groove dimensions (i.e. width x depth), that is, 8 × 8 mm, 10 × 10 and 12 × 12 mm with 1.33, 1.67 and 2.00 groove width or depth to FRP bar diameter (b/db) were considered.

The retrofitting design of tested specimens are provided in Table 1. The designation of the specimens followed the format "X-Y", while X indicates the FRP type (i.e. C for CFRP, G for GFRP and B for BFRP) and Y is the groove size (i.e. 8, 10 or 12). It's noteworthy that the word "Edge" was added after Y for the specimens retrofitted with FRP installed at the groove edge, while using the letters "D" or "T" after Y indicates the specimens retrofitted with two or three FRP bars (doubled or tripled number of bars), respectively. An exception was made to those specimens retrofitted with NE only, as there were designated NE-8.

2.2. Material properties

2.2.1. Concrete

Concrete with 28-day average compressive strength of 29.6 MPa, determined on standard concrete cylinders (i.e. 100 mm diameter × 200 mm height), was prepared. Concrete mix design is listed in Table 2.

2.2.2. FRP reinforcement

CFRP, GFRP and BFRP round bars with 6 mm diameter were used for the purpose of this study. The FRP bars are shown in Fig. 1b and their mechanical properties are provided in Table 3. The CFRP bars were

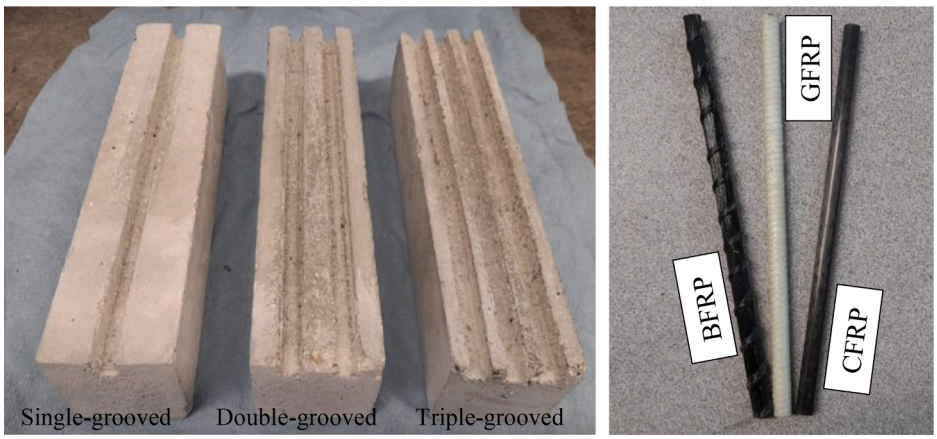

Fig. 1. (a) Concrete specimens to be retrofitted and (b) FRP bars used in this study.

Table 1
NSM-FRP retrofitting design.

Specimen	FRP reinforcement	Groove dimensions (mm^2)	FRP bar position	Number of FRP bars
Control	–	–	–	–
NE-8	–	8 × 8	–	–
C-8	CFRP	8 × 8	Centre	One
G-8	GFRP			
B-8	BFRP			
C-10	CFRP	10 × 10		
C-12	CFRP	12 × 12		
G-10	GFRP	10 × 10		
G-10-Edge	GFRP	10 × 10	Edge	
G-12-Edge	GFRP	12 × 12	Edge	
C-8-D	CFRP	8 × 8	Centre	Two
C-8-T	CFRP			Three

Table 2
Concrete mix design.

C: S: Agg. = 1:1:2 (by volume) Ingredient	Description	Quantity (Kg/m^3) ($w/c = 0.50$)
Cement	Type I Ordinary Portland cement (OPC)	340
Coarse aggregate	Crushed stones with angular edges (1 mm < size < 5 mm)	780
Sand	Sharp silica sand with uniform grain size (250 μm < size < 1 mm)	397.5
Water	Tap water	170

Table 3
Mechanical properties of the FRP bars and epoxy adhesive (As per suppliers).

Property Material	Tensile strength (MPa)	E-modulus (GPa)	Elongation at break (%)
CFRP (Sika® CarboDur® BC 6)	3100	148	1.6
GFRP	1280	> 40	N/A
BFRP	1000	≥ 45	N/A
Epoxy adhesive	29	11.2	N/A

provided by Sika Limited, UK, while Engineered Composites Ltd, UK provided the GFRP and the BFRP bars.

2.2.3. Epoxy adhesive

Sikadur®−30, a thixotropic, structural 2-component adhesive, based on a combination of epoxy resin and hardener (i.e. A & B) was used. Properties of epoxy are shown in Table 3. Epoxy was provided by Sika Limited, UK.

2.3. Retrofitting process and test setup

The NSM-FRP retrofitting process started with roughening the groove sides with sandpaper. Then, an air compressor was used to clean and remove the dust from the grooves. After adhesive was put partly into the grooves using a trowel, the FRP bars were placed in the grooves and carefully pressed. This helped the paste spread around the strip and fill the gap between the bars and the groove sides. Finally, more adhesive was added to the grooves, and the surface was levelled. The retrofitted specimens were then air-cured in the ambient temperature for 7 days. This ensured that the adhesive properly cured and created a sufficient bond between the concrete substrate and the FRP reinforcement bars. The retrofitting process is depicted in Fig. 2. The specimens were tested using an INSTRON 5969 Universal testing machine under a 150 kN load cell with a crosshead speed of 1.04 MPa/min (avg.) according to the ASTM C 78–02 [26]. The ultimate loads, flexural strength and displacements at maximum loads (described as maximum displacements through the paper) were recorded using a data acquisition system, and the failure modes were also monitored.

3. Results and discussion

A total of 36 three-point bending tests were conducted, three replicates (i.e. A, B and C) of each configuration were prepared and the average capacities (i.e. ultimate loads, max flexural strength and the maximum displacement (i.e. ductility)) were obtained and are summarised in Table 4. The failure mode of each replicate was addressed individually. The effect of the different parameters on the overall flexural capacities, ductility and the failure modes of the retrofitted concrete are discussed in the following sections.

3.1. The effect of presence of FRP reinforcement

3.1.1. Overall flexural capacity

It was observed that retrofitting concrete by epoxy only (i.e. NE-8) resulted in about 38 % and 2 % increase in the ultimate load and

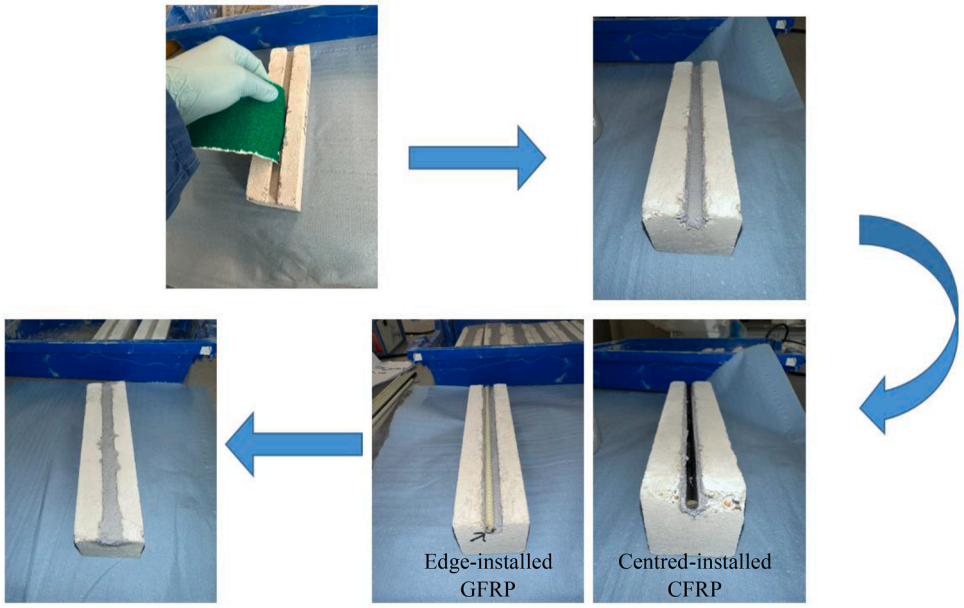

Fig. 2. NSM-FRP retrofitting of concrete specimens.

Table 4
Overall capacities and failure modes of tested specimens.

Specimen	Avg. ultimate load (kN) (CoV*)	Avg. max flexural strength (MPa)	Avg. max displacement (mm) (CoV)	Failure mode
Control	3.55 (0.08)	6.39	0.58 (0.17)	Flexural
NE-8	4.90 (0.06)	8.81	0.59 (0.32)	Flexural
C-8	14.75 (0.04)	26.55	1.27 (0.09)	Shear and debonding
G-8	14.86 (0.07)	26.75	1.84 (0.12)	Flexural
B-8	14.85 (0.19)	26.73	2.02 (0.05)	Shear and flexural
C-10	21.67 (0.16)	38.99	1.61 (0.11)	Shear
C-12	12.98 (0.13)	23.37	1.84 (0.12)	Shear and concrete crushing
G-10	14.36 (0.19)	25.85	2.63 (0.24)	Shear and flexural
G-10-Edge	14.56 (0.20)	26.21	2.00 (0.26)	Shear and flexural
G-12-Edge	13.10 (0.20)	23.58	2.49 (0.25)	Shear and flexural
C-8-D	17.80 (0.09)	32.04	3.06 (0.81)	Debonding and FRP rupture
C-8-T	24.96 (0.06)	44.94	2.12 (0.19)	Debonding

* Coefficient of variation.

ductility, respectively over the non-retrofitted specimen. The capacity increase may be due to the high tensile strength of epoxy compared to that of concrete, which enhanced the flexural capacity of concrete specimens. On the other hand, using such brittle adhesive had a trivial effect on the ductility. While using CFRP, GFRP or BFRP bars alongside NE resulted in about 315 %, 319 % and 318 % increase in the ultimate loads, respectively with accompanying 119 %, 217 % and 248 % ductility increase over the control specimen.

In comparison with specimen NE-8, it was found that using CFPR bars combined with NE (i.e. specimen C-8) for retrofitting showed about 201 % increase in the load-carrying capacity of the specimens and about 115 % in ductility. Retrofitting specimens with GFRP bars resulted in about 203 % and 212 % ultimate load and ductility increases, respectively, while the BFRP-retrofitted specimens showed about 203 % and 242 % increases, respectively in the ultimate load and ductility. It is apparent that using the FRP reinforcement alongside epoxy would resist the crack progression in addition to enhance the bond at the interfaces, which would eventually delay the failure. It was also noticed that using different types of FRP bars had a similar contribution (i.e. increase) in the load-bearing capacities, but different ductility response was observed. This could be due to the difference in the mechanical properties of FRPs (Table 3), which affected the bond behaviour of the interfaces, and ultimately the specimens' ductility. The test results are shown in Fig. 3.

3.1.2. Failure modes

As shown in Fig. 4, using NE alone for retrofitting resulted in a brittle failure mode, as it resulted in an insignificant improvement in the ductility of the retrofitted concrete, as discussed in the previous section. Thus, the flexural crack can be seen to easily propagate through the epoxy line passing to the other side of concrete substrate, breaking the specimens into two parts. While in the case of considering FRP reinforcement bars in the retrofitting process, the modes of failure seemed to be more ductile, and they changed to shear failure mode combined with bar slippage in the CFRP-retrofitted specimens, while the specimens retrofitted with GFRP bars mainly failed in flexure, which resulted in peeling-off of the adhesive layer at the bar-epoxy interface followed by a partial detachment of concrete substrate. A mixed shear and flexural failure mode was observed in the BFRP-retrofitted specimens, leading to minor concrete crushing.

It's worth mentioning that, owing to the comparatively lower mechanical properties of the BFRB bars (Table 3), the BFRP-retrofitted specimens exhibited a higher degree of ductility. This enhanced ductility was manifested through the presence of a greater number of minor cracks around the concrete-adhesive interface prior to failure, which contrasted with the behaviour observed in the GFRP-retrofitted specimens. The latter, on the other hand, demonstrated a higher incidence of hairline cracks (i.e. higher ductility) before reaching the failure point compared to specimens retrofitted with CFRP bars, known for their superior mechanical properties.

3.2. The effect of position of FRP reinforcement

3.2.1. Overall capacity

Test results exhibited that changing the position of the GFRP bars

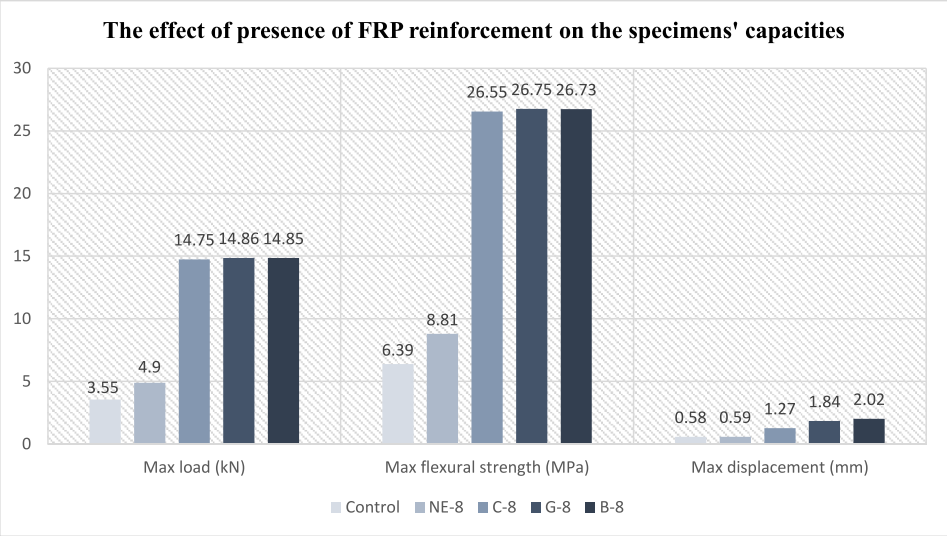

Fig. 3. Effect of presence of FRP reinforcement on the specimens' capacities.

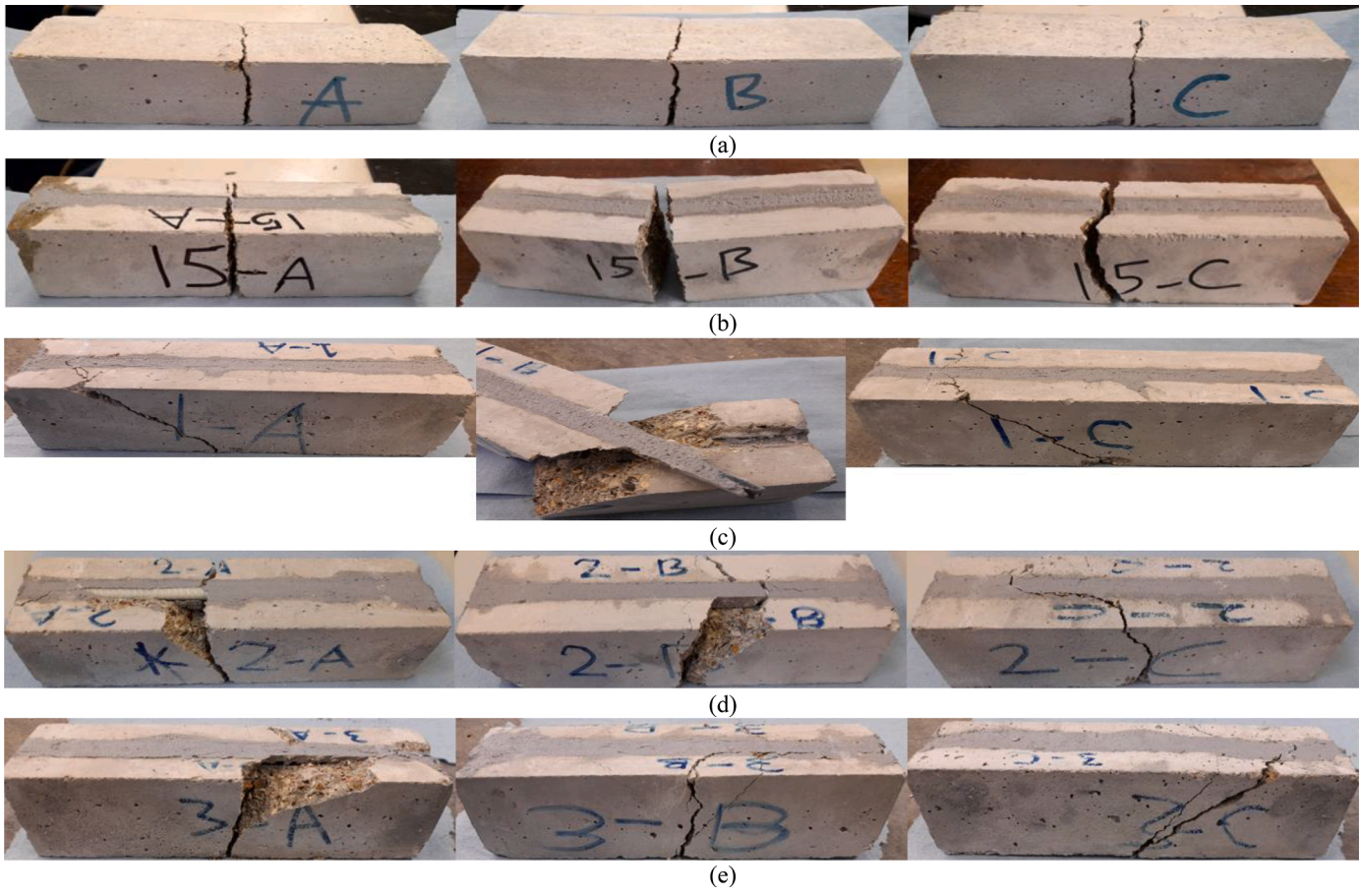

Fig. 4. Failure modes of specimens (a) control, (b) NE-8, (c) C-8, (d) G-8 and (e) B-8.

inside the grooves had trivial effect on the load-carrying capacities of the specimens, where only about 1 % capacity increase was observed with considering the edge-installed reinforcement over the centred-installed one. However, a considerable increase of about 32 % in the ductility was observed by the latter configuration over the former one. This could be because of in the case of the edge-installed FRP bar the thickness of the epoxy layer between the bar and the concrete substrate at that edge was less compared to that in the case of the middle-installed bar, and as the epoxy layer acts as a medium to transfer stress from concrete to FRP, thinner epoxy layer might not be able to work properly (i.e. transfer stress) amongst the interfaces as it did in the other specimen, which eventually increased the stress concentration at the edge leading the specimen to behave in more brittle mode. Fig. 5 shows the results graphically.

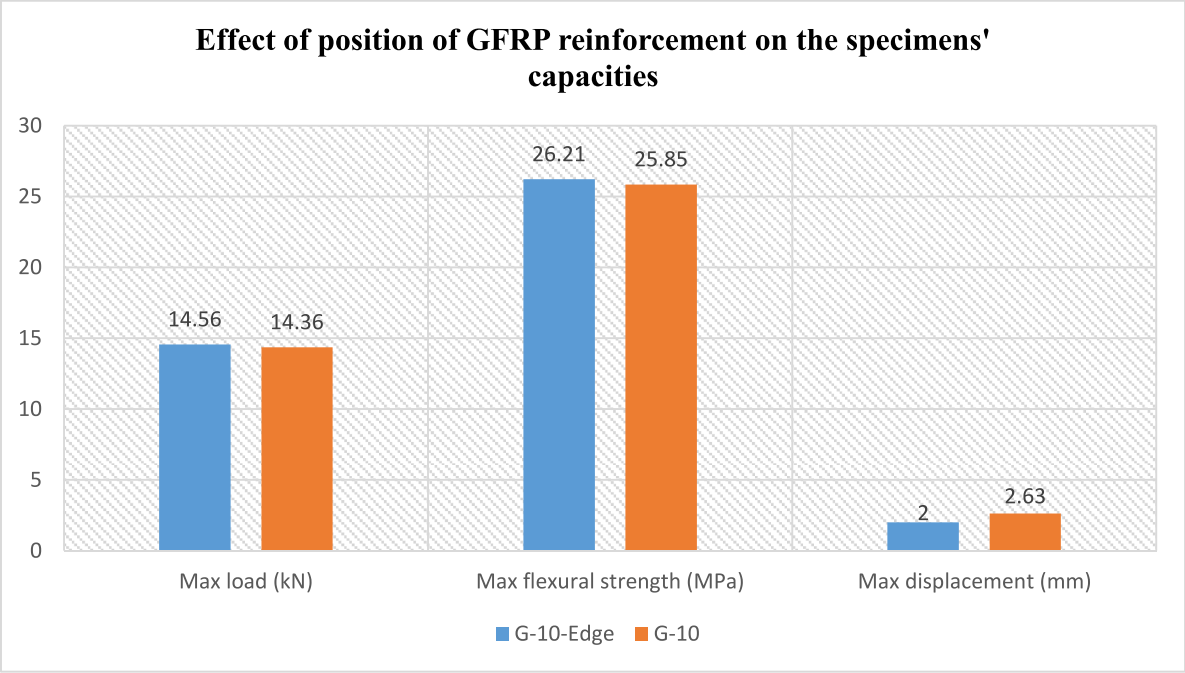

Fig. 5. Effect of position of GFRP reinforcement on the specimens' capacities.

3.2.2. Failure modes

A combined shear and flexural mode of failure was noticed in specimen G-10. Where specimens A and B mainly failed in flexure, as a wide flexural crack produced in the middle of the specimens breaking through the epoxy line to the other side, however, no debonding was observed. A minor shear crack appeared to the right of the main crack, but it did not contribute to the failure mode. Specimen C failed due to a major shear crack, leading to peeling-off of a small part of concrete and epoxy layer at the epoxy-FRP interface (i.e. debonding), however no minor cracks were noticed.

Similar observations were reported in specimen G-10-Edge, in which specimens A and B failed in pure flexure with one main crack produced and progressed through concrete and directly moved to pass through the entire epoxy layer to the other side without generating a crack tail along the epoxy line, which also occurred in specimen G-10. Specimen G-10-Edge-C failed in similar manner to that noticed in specimen G-10-C, but no debonding or concrete detachment took place in the former specimen. This was attributed to that, as previously discussed, putting the FRP bar at the groove edge decreased the specimens' ductility, which could lead to premature failure before any type of peeling-off happens. In addition, being the bar closer to the concrete edge, this might protect it, to some extent, from debonding, as stresses might not be able to progress into the concrete body. The failure modes of specimens G-10 and G-10-Edge are shown in Fig. 6.

3.3. The effect of number of CFRP reinforcement bars

3.3.1. Overall capacity

Increasing the amount of the CFRP reinforcement resulted in an enhancement in the load-carrying capacities in addition to the ductility response. Where doubling the number of the CFRP bars yielded about 21 % and about 141 % increases in the ultimate load and ductility, respectively, about 69 % capacity increase and about 67 % ductility enhancement were obtained with tripling the number of bars. Moving from two to three bars was found to increase the capacity by about 40 %, however, about 44 % reduction in the ductility was remarked.

It could be axiomatic to obtain a capacity increase with increasing the number of bars, which would enhance the resistance to failure cracking and eventually delay the failure. However, the ductility improvement could be referred to that using more reinforcement would make the crack progression more difficult, as the crack in the single FRP-retrofitted specimens, for instance, would need to break though only one adhesive layer to cause the failure at the interface and eventually in the specimen, but in the case of the presence of two or three adhesive layers,

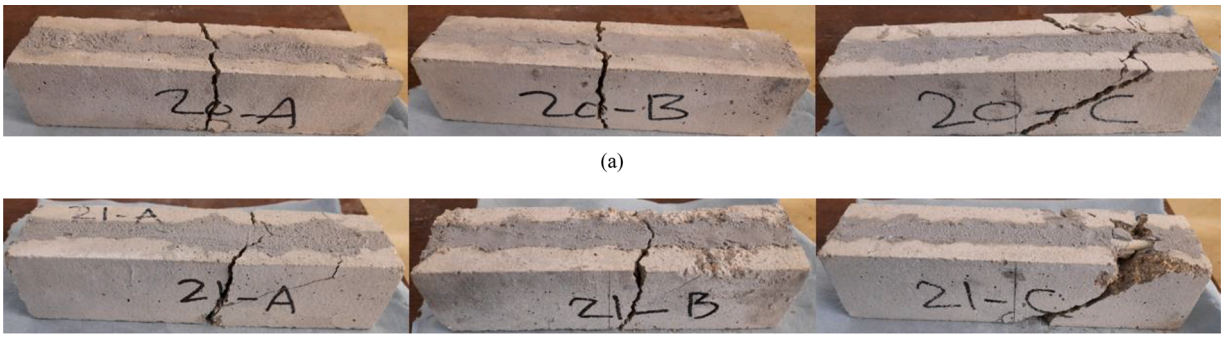

Fig. 6. Failure modes of specimens (a) G-10-Edge and (b) G-10.

the task would be harder and would take longer to be achieved. This would end up with higher-strength specimens and result in a more ductile behaviour, since the specimen would keep displaced for longer time. Nevertheless, increasing the number of FRP bars by 50 % (i.e. from two bars to three) negatively affected the average ductility of the retrofitted concrete, as found in some previous studies [21,27]. The results are shown in Fig. 7.

3.3.2. Failure modes

It is evident that the specimens C-8 (i.e. A, B and C) mainly failed in shear. Where in specimen A, the shear crack produced in the concrete body and continued to pass through the epoxy layer but with less width than in the concrete, since epoxy is stronger, which was able to stop its progress. Similar mode of failure was noticed in specimen C, but the crack continued to progress through concrete after it passed the epoxy layer, which was able to curb the crack to pass through it in specimen B, but that led to debonding (i.e. CFRP bar slippage) at the FRP-epoxy interface. A shear failure followed by debonding at the bar-epoxy interface was noticed in specimen C-8-D-A, in addition to CFRP rupture. While debonding at both the concrete-epoxy and epoxy-bar interfaces was noticed in specimens B and C, with partial concrete detachment in C, no minor cracks were remarked in C-8 and C-8-D. For specimen C-8-T, it was noticed that A, B and C failed in the same manner, which was due to shear cracks that eventually led to debonding at both interfaces. Some minor cracks showed up near the surface. The failure modes of specimens C-8-D and C-8-T are shown in Fig. 8.

Therefore, the increase in the number of CFRP bars resulted in the retention of the shear failure mode within the concrete structures. However, an increase in debonding at the interfaces was observed, potentially attributable to inadequate clear groove spacing and clear edge distance. The insufficiency in clear groove spacing and edge distance can lead to a reduced bonding area between the CFRP bars and the concrete substrate, consequently promoting the debonding mechanism and impacting the overall effectiveness of the retrofitting process.

3.4. The effect of groove dimensions

3.4.1. Overall capacity

The groove size had a significant influence on the performance of retrofitted concrete depending on the type of FRP. The CFRP-retrofitted concrete with the groove size 10 × 10 mm^2 yielded a significant increase in the load-carrying capacity and ductility than that with 8 × 8 mm^2 groove size, about 47 % and 27 %, respectively, which disagrees with what was reported in the literature [17,21]. Further increase in the groove dimensions (i.e. using 12 × 12 mm^2 grooves) led to capacity drops by about 14 % and 67 % compared to using 8 × 8 and 10 × 10 mm^2 grooves, respectively. Nevertheless, corresponding increases in the specimens' ductility of about 45 % and 14 % were remarked.

Therefore, increasing the groove size (in mm^3) by about 56 % (i.e. from 8 × 8 × 200 to 10 × 10 × 200) with keeping the same FRP dimensions means that more adhesive was utilised. Moreover, increasing the groove size means installing the FRP reinforcement further to the groove border, which would delay the stresses generated in the specimen from affecting the FRP-adhesive interface, which would eventually delay the failure, and end up with a higher-capacity specimen. Furthermore, it was reported by Hassan and Rizkalla [23] that increasing the thickness of the adhesive (i.e. by increasing the groove) would reduce the stress deformation within the adhesive layer, which would eventually reduce the interfacial stresses. However, further increasing in the groove size resulted in a reverse effect, as a sharp drop in the capacity was reported. This might be due to that too much adhesive negatively affected the interfacial adhesion, leading to a premature failure.

It was also observed that the ductility of the retrofitted concrete increased with the groove size. This could be due to that increasing the groove dimensions, which means increasing the distance between two groove sides might delay the crack progression, which would take longer to cross from one to another side causing the failure, leading to more ductile behaviour. The results are represented graphically in Fig. 9(a).

Contrary to what was observed in the CFRP-retrofitted concretes, moving from 8 × 8 to 10 × 10 mm^2 in the GFRP-retrofitted concretes yielded a slight (about 3 %) reduction in the capacity. This might be due to the difference in the mechanical properties (i.e. the tensile strength) of the bars, which could affect the behaviour, as the other components (i.e. epoxy and concrete) did not vary. However, about 43 % ductility increase was achieved, which was due to the same reasons mentioned earlier. The results are presented graphically in Fig. 9(b).

It was also remarked that increasing the groove dimensions from 10

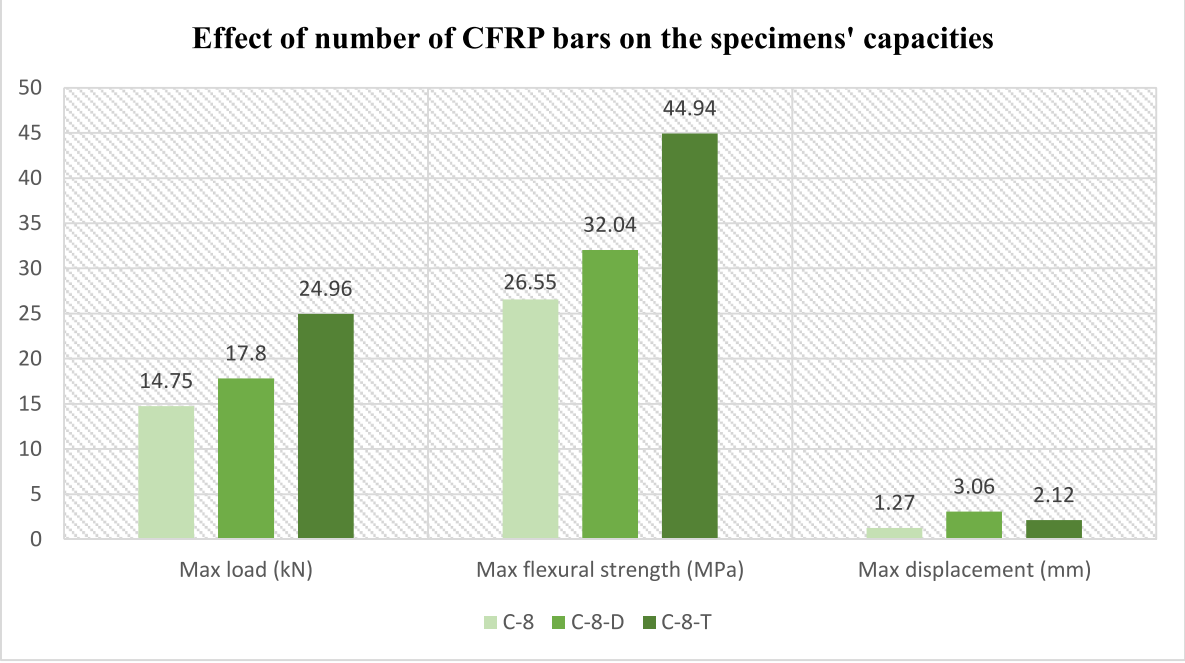

Fig. 7. Effect of the number of the CFRP bars on the specimens' capacities.

(a)

(b)

Fig. 8. Failure modes of specimens (a) C-8-D and (b) C-8-T.

$\times$ 10 to 12 $\times$ 12 mm^2 in the specimens retrofitted with edge-installed GFRP bars led the load-carrying capacity to decrease by about 11 %, however, about 25 % ductility increase was observed. This could be ascribed to the same reasons reported in the previous group of specimens. Fig. 9(c) shows the results graphically.

3.4.2. *Failure modes*

It can be seen that the specimen C-8, as discussed in section earlier, mainly failed due to shear. The shear crack produced in the concrete body passing through the epoxy layer causing a normal shear failure in specimens A and C, but leading to debonding failure at the FRP-epoxy interface resulting in CFRP bar slippage.

Specimen C-10 had almost the same failure modes that took place in specimens A and B, as a main shear crack produced in the middle of the specimens from the bottom and kept progressing to break through the epoxy layer with a short tail along the edge of the epoxy line until, eventually, broke through it to the other side. Similar details were observed in specimen C, but one more shear crack generated with longer tail, but it kept beside the epoxy line without passing through it. No debonding was remarked in any of the specimens, which could be due to, as reported by De Lorenzis and Nanni [24,25], that as the groove size increased, the thickness of the epoxy cover increased, which offered a higher resistance to splitting and eventually shifted the failure from epoxy to the surrounding concrete.

Similarly, the retrofitted concretes, C-12 (A, B and C) failed in shear, where a major shear crack began created and progressed through concrete without breaking through the adhesive layer, but it kept progressing align to it leading, eventually, to a complete debonding failure at the concrete-adhesive interface with a partial concrete crushing. Some additional cracks also generated in specimens A and C. Failure modes of specimens C-10 and C-12 are shown in Fig. 10(a) and (b), respectively.

For the GFRP-retrofitted specimens, flexural failure was the dominant in specimens G-8. In specimen A, the flexural crack generated into concrete could break through the adhesive layer, and also kept progressing align to the GFRP-epoxy interface resulting in a partial peeling-off of the epoxy layer at the bar-epoxy interface and causing a part of concrete to detach. Specimen B failed by approximately the same manner, but the epoxy layer did not peel off. Similar observations were reported in specimen C, but the major crack that caused the failure was narrower than those appeared in the previous specimens. Specimen G-10, as discussed earlier, failed in a combined flexural and shear failure mode. Where specimens A and B mainly failed in flexure, while shear failure was the dominant in specimen C, leading to a partial concrete detachment followed by debonding at the bar-epoxy interface.

For the specimens retrofitted with edge-installed GFRP bars, specimens A and B of G-10-Edge, as mentioned earlier, showed a pure flexure failure mode, while specimen C mainly failed in shear. Specimens G-12-Edge-A and C failed in the same manner, as a flexural crack generated in the concrete and continuing align to the epoxy line, without causing concrete detachment. Contrary to that, part of concrete was noticed to peel off in specimen B, which failed due to a major shear crack produced in the concrete body and continued to progress at the edge of the adhesive layer. Failure mode of specimen G-12-Edge is shown in Fig. 10(c).

4. Conclusions

The effectiveness of the NSM-FRP retrofitting of concrete prisms has been thoroughly examined with variation of the presence, position and number of FRP bars, in addition to the groove size. These parameters were studied for their effect on the specimens' performance, including the load-carrying capacities (i.e. ultimate load and maximum flexural strength), ductility and modes of failure. From the obtained results, the following conclusions could be drawn:

- Retrofitting specimens with NE only increased the capacity and ductility by about 38 % and 2 %, respectively over the non-retrofitted specimens. No change on the mode of failure (i.e. flexural) was noticed.
- Using CFRP, GFRP and BFRP reinforcement bars with NE achieved about 201 %, 203 % and 203 % increases in the load-carrying capacities, respectively with accompanying 115 %, 212 % and 242 % ductility increases in ductility over those retrofitted with NE only.

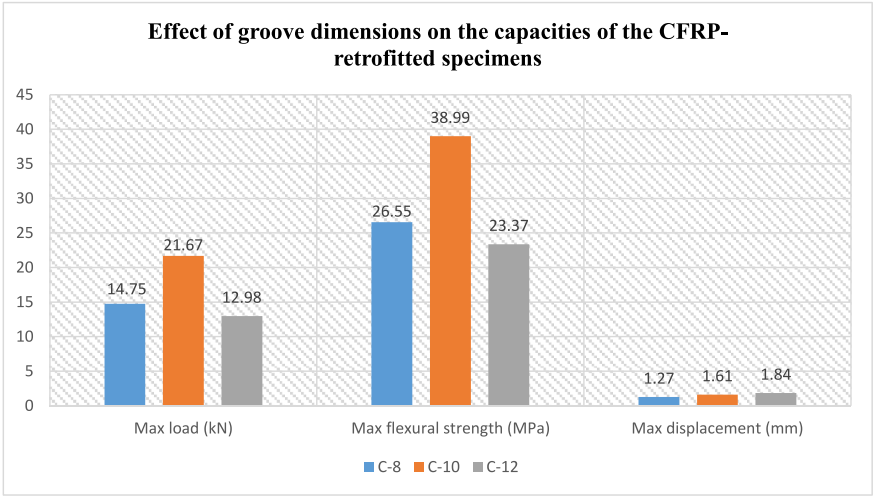

(a)

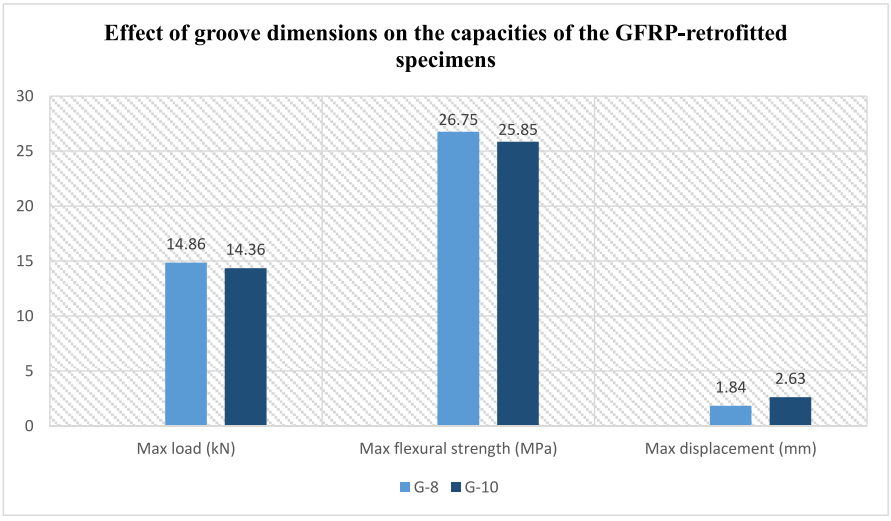

(b)

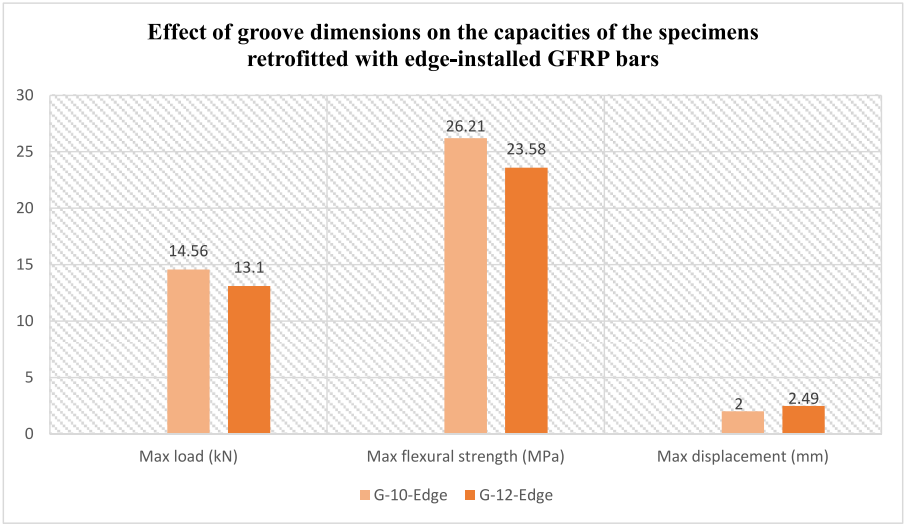

(c)

Fig. 9. Effect of groove dimensions on the capacities of the specimens retrofitted with (a) CFRP bars and (b) GFRP bars and (c) edge-installed GFRP bars.

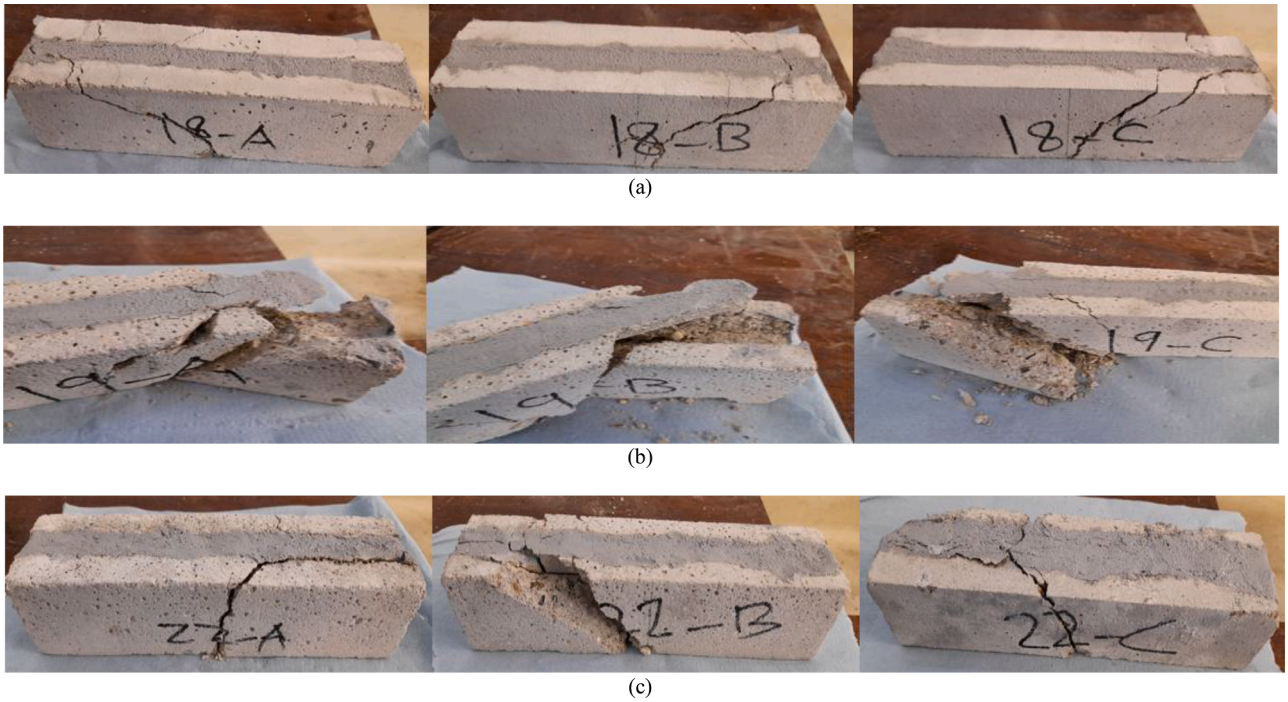

Fig. 10. Failure modes of specimens (a) C-10, (b) C-12 and (c) G-12-Edge.

- Using FRP reinforcement with NE rather than NE only resulted in more ductile failure mode, in addition to significantly improving the resistance to the crack progression.
- Installing the GFRP reinforcement at the edge of the groove rather than in the centre had a trivial effect on the load-carrying capacity, but decreased the ductility by about 24 %, which could be due to the increase in the stress concentration at the interfaces.
- The debonding at the bar-epoxy interface and the concrete detachment could be avoided by installing the GFRP reinforcement at the groove edge instead of at its centre, as the bar was closer to the concrete substrate and was protected by it.
- Doubling and tripling the number of the CFRP bars led, respectively to about 21 % and 69 % increases in the load-carrying capacities, with accompanying ductility increases of about 141 % and 67 %. While about 40 % capacity increase was obtained when moving from two to three bars, however, about 44 % ductility drop was observed.
- Increasing the number of the CFRP bars kept the shear failure mode, but increased the debonding at the interfaces, which could be due to the insufficient clear groove spacing and the clear edge distance.
- Using the groove size in the CFRP-retrofitted specimens of 1.67db instead of 1.33db increased the capacities of the retrofitted concretes by about 47 %, but using size of 2.00db resulted in a about 14 % capacity reduction. Nevertheless, an increase in the ductility was found to follow the increase in the groove size.
- All CFRP-retrofitted specimens failed in shear. A bar-epoxy debonding failure was noticed in one of the 8 mm-grooved specimens but a debonding at the concrete-adhesive interface occurred in all the 12 mm-grooved ones, while debonding could be completely avoided in the 10 mm-grooved specimens.
- For the specimens retrofitted with centred-installed GFRP bars, increasing the groove size from 1.33 db to 1.67 db slightly decreased the capacities, but about 30 % increase in the ductility was achieved.
- Changing the groove size from 1.67db to 2.00db in the specimens retrofitted with edge-installed GFRP bars led to about 11 % capacity decrease, but about 25 % ductility enhancement was observed.
- Changing the groove size in the GFRP-retrofitted specimens (i.e. centred-installed) had an insignificant effect on the failure modes. While specimens retrofitted with edge-installed GFRP bars (i.e. G-10-Edge and G-12-Edge) exhibited combined shear and flexural failure modes. Partial concrete detachment occurred only in the latter specimen.

Declaration of Competing Interest

The authors declare that they have no known competing financial interests or personal relationships that could have appeared to influence the work reported in this paper.

Data availability

Data will be made available on request.

References

[1] N.T.K. Al-Saadi, A. Mohammed, R. Al-Mahaidi, J. Sanjayan, A state-of-the-art review: near-surface mounted FRP composites for reinforced concrete structures, Constr. Build. Mater. 209 (2019) 748–769.
[2] Z.E.A. Benzeguir, G. El-Saikaly, O. Chaallal, Size effect in RC T-beams strengthened in shear with externally bonded CFRP sheets: experimental study, J. Compos. Constr. 23 (6) (2019), 04019048.
[3] M. Ibrahim, T. Wakjira, U. Ebead, Shear strengthening of reinforced concrete deep beams using near-surface mounted hybrid carbon/glass fibre reinforced polymer strips, Eng. Struct. 210 (2020), 110412.
[4] J.H. Gonzalez-Libreros, C. Sabau, L.H. Sneed, C. Pellegrino, G. Sas, State of research on shear strengthening of RC beams with FRCM composites, Constr. Build. Mater. 149 (2017) 444–458.
[5] C.E. Bakis, L.C. Bank, V. Brown, E. Cosenza, J.F. Davalos, J.J. Lesko, A. Machida, S. H. Rizkalla, T.C. Triantafillou, Fiber-reinforced polymer composites for construction—State-of-the-art review, J. Compos. Constr. 6 (2) (2002) 73–87.
[6] S.J.E. Dias, J.A.O. Barros, Shear strengthening of RC T-section beams with low strength concrete using NSM CFRP laminates, Cem. Concr. Compos. 33 (2) (2011) 334–345.
[7] S.J. Dias, J.A. Barros, Shear strengthening of RC beams with NSM CFRP laminates: experimental research and analytical formulation, Compos. Struct. 99 (2013) 477–490.
[8] S.J. Dias, J.A. Barros, NSM shear strengthening technique with CFRP laminates applied in high T cross section RC beams, Compos. B. Eng. 114 (2017) 256–267.
[9] M. Al-Zu'bi, M. Fan, Y. Al Rjoub, A. Ashteyat, M.J. Al-Kheetan, L. Anguilano, The effect of length and inclination of carbon fiber reinforced polymer laminates on shear capacity of near-surface mounted retrofitted reinforced concrete beams, Struct. Concr. 22 (6) (2021) 3677–3691.

[10] S.S. Zhang, T. Yu, G.M. Chen, Reinforced concrete beams strengthened in flexure with near-surface mounted (NSM) CFRP strips: current status and research needs, Compos. B Eng. 131 (2017) 30–42.
[11] F. Al-Mahmoud, A. Castel, R. François, C. Tourneur, Strengthening of RC members with near-surface mounted CFRP rods, Compos. Struct. 91 (2) (2009) 138–147.
[12] W.C. Tang, R.V. Balendran, A. Nadeem, H.Y. Leung, Flexural strengthening of reinforced lightweight polystyrene aggregate concrete beams with near-surface mounted GFRP bars, Build. Environ. 41 (10) (2006) 1381–1393.
[13] A. Siddika, M.A. Al Mamun, W. Ferdous, R. Alyousef, Performances, challenges and opportunities in strengthening reinforced concrete structures by using FRPs–A state-of-the-art review, Eng. Fail. Anal. 111 (2020), 104480.
[14] I.A. Sharaky, L. Torres, J. Comas, C. Barris, Flexural response of reinforced concrete (RC) beams strengthened with near surface mounted (NSM) fibre reinforced polymer (FRP) bars, Compos. Struct. 109 (2014) 8–22.
[15] T. Hassan, S. Rizkalla, Bond mechanism of NSM FRP bars for flexural strengthening of concrete structures, J. Am. Concr. Inst. 101 (6) (2004) 830–839.
[16] Y. Zhang, M. Elsayed, L.V. Zhang, M.L. Nehdi, Flexural behavior of reinforced concrete T-section beams strengthened by NSM FRP bars, Eng. Struct. 233 (2021), 111922.
[17] S.M. Soliman, E. El-Salakawy, B. Benmokrane, Flexural behaviour of concrete beams strengthened with near surface mounted fibre reinforced polymer bars, Can. J. Civ. Eng. 37 (10) (2010) 1371–1382.
[18] M.N. Nurbaiah, A.H. Hanizah, A. Nursafarina, M.N. Ashikin, Flexural behaviour of RC beams strengthened with externally bonded (EB) FRP sheets or Near Surface Mounted (NSM) FRP rods method, in: 2010 International Conference on Science and Social Research (CSSR 2010), IEEE, 2010, pp. 1232–1237.
[19] S.M. Daghash, O.E. Ozbulut, Flexural performance evaluation of NSM basalt FRP-strengthened concrete beams using digital image correlation system, Compos. Struct. 176 (2017) 748–756.
[20] H.M. Ali, M.N. Sheikh, M.N. Hadi, Flexural strengthening of RC beams with NSM-GFRP technique incorporating innovative anchoring system, Structures 38 (2022) 251–264.
[21] S.W. Fathuldeen, M.A. Qissab, Behavior of RC beams strengthened with NSM CFRP strips under flexural repeated loading, Insights Innovations Struct.. Eng., Mech. Comput., Proc. Int. Conf., 6th 70 (1) (2019) 67–80.
[22] K. Sanginabadi, A. Yazdani, D. Mostofinejad, C. Czaderski, RC members externally strengthened with FRP composites by grooving methods including EBROG and EBRIG: a state-of-the-art review, Constr. Build. Mater. 324 (2022), 126662.
[23] T. Hassan, S. Rizkalla, Investigation of bond in concrete structures strengthened with near surface mounted carbon fiber reinforced polymer strips, J. Compos. Constr. 7 (3) (2003) 248–257.
[24] L. De Lorenzis, A. Nanni, Bond between near-surface mounted fiber-reinforced polymer rods and concrete in structural strengthening, Struct. J. 99 (2) (2002) 123–132.
[25] L.D. Lorenzis, A. Nanni, Characterization of FRP rods as near-surface mounted reinforcement, J. Compos. Constr. 5 (2) (2001) 114. -12.
[26] ASTM, C., Standard test method for flexural strength of concrete (using simple beam with third–point loading). Annual Book of ASTM Standards, American Society for Testing and Materials, 2002, p. 78.
[27] M. Abdallah, F. Al Mahmoud, A. Khelil, J. Mercier, B. Almassri, Assessment of the flexural behavior of continuous RC beams strengthened with NSM-FRP bars, experimental and analytical study, Compos. Struct. 242 (2020), 112127.
[28] ACI Committee 440.2R-08, Guide For the Design and Construction of Externally Bonded FRP Systems for Strengthening Concrete Structures, American Concrete Institute, Farmington Hills, Michigan, USA, 2008.